EVS27
Barcelona, Spain, November 17-20, 2013

Development of Wide Range High Efficiency for Electric Propulsion System

Kun-Lun Chuang, Yong-Kai Lin, Shin-Hung Chang and Bo-Tseng Sung

Mechanical and Systems Research Laboratories, Industrial Technology Research Institute,

195, Sec 4, Chung Hsing Rd., Chutung, Hsinchu, Taiwan, R. O. C.,

KLChuang@itri.org.tw

Abstract

This study focuses on development of a control strategy for a 50kW permanent magnet synchronous motor (PMSM). Through above-mentioned control strategy, the performance of PMSM can be enhanced for wide speed ranges high efficiency. In this paper, vector control is implemented based on feed-forward current control strategy. Therefore, the feature of the proposed control scheme is to improve performance of the proportional- integral (PI) current control, including overshoot, transient response time and parameters tuning time. Finally, the effectiveness of the proposed control strategy for 50kW PMSM is verified by experimental results.

Keywords: PMSM, vector control, feed-forward current control, proportional- integral current control.

1 Introduction

In recent years, home application industry continuously requires high efficiency power electrical machine because of increasing demand of energy and environmental issues. The more energy and environmental regulations have been enhanced, the more various efforts to suppress increasing product cost have been attempted. Due to the advantages of small size, light weight, fast response and high efficiency, permanent magnet synchronous motor (PMSM) is widely used in aviation and aerospace, military, industrial and agricultural areas [1].

On the other hand, vector control clearly requires instantaneous control of stator current. Vector control usually realized with digital PWM controller in rotating (d-q) reference frame of vector control is to control flux and torque of machine to drive the motor to accurately trace the reference command value irrespective of load, machine parameter and any external environmental changes. In vector control stator current is controlled instantaneously which reduces the torque ripples and improves overall performance of machine [2]. Vector control PMSM drives decouples torque, flux and it also makes the control quite easier. Consequently, vector control becomes the core control strategy of PMSM.

In general, conventional proportional-integral-differential (PID)-type controllers have been widely used in industry due to their simple control structure, ease of design, and inexpensive cost. However, the PID-type controller can not provide perfect control performance if the controlled plant is highly nonlinear and uncertain. The motivation of this study is to design a real-time control scheme that possesses the evolutionary capability of the feed-forward current control strategy [3].

2 Dynamic model of PMSM

Mathematical modeling of motor is required for simulation and analysis of drive system. PMSM equations are presented in d-q reference frame [4]. The stator flux-linkage equations are given by:

$$V_{qs} = r_s i_{qs} + \frac{d\lambda_{qs}}{dt} + \omega_e \lambda_{ds} \qquad (1)$$

$$V_{ds} = r_s i_{ds} + \frac{d\lambda_{ds}}{dt} - \omega_e \lambda_{qs} \quad (2)$$

where ω_e is the electrical angular velocity, r_s is the stator resistance for per-phase, i_{qs} and i_{ds} are the d-q axes stator currents, respectively, V_{qs} and V_{ds} are the d-q axes stator voltages, respectively, λ_{ds} and λ_{qs} are flux linkages, respectively.

The d and q axes Flux Linkages in rotor reference frame are given by

$$\lambda_{qs} = L_s i_{qs} + L_m i_{qr} \quad (3)$$

$$\lambda_{ds} = L_s i_{ds} + L_m i_{dr} \quad (4)$$

The PM excitation can be modeled as a constant current source i_{fr}. The rotor flux is along the d-axis, so the d-axis rotor current is i_{fr}. The q-axis current in the motor is zero, because there is no flux along this axis in the rotor, by assumption

$$\lambda_{qs} = L_{qs} i_{qs} + L_m i_{qr} \quad (5)$$

$$\lambda_{ds} = L_{ds} i_{ds} + L_m i_{dr} + L_m i_{fr} \quad (6)$$

where L_m is mutual inductance between the stator winding and rotor magnets.

Above voltage equations can be represented in matrix form as given below

$$\begin{bmatrix} V_{qs} \\ V_{ds} \end{bmatrix} = \begin{bmatrix} r_s + sL_{qs} & \omega_e L_{ds} \\ -\omega_e L_{qs} & r_s + sL_{ds} \end{bmatrix} \begin{bmatrix} i_{qs} \\ i_{ds} \end{bmatrix} + \begin{bmatrix} \omega_e \lambda_f \\ 0 \end{bmatrix} \quad (7)$$

This is the dynamic model of PMSM used in vector control. The developed torque motor is being given by

$$T_e = \frac{3}{2}\frac{p}{2}(\lambda_{ds} i_{qs} - \lambda_{qs} i_{ds}) \quad (8)$$

Use (5) and (6) into (8) can be rewritten as

$$T_e = \frac{3}{2}\frac{p}{2}[L_m(i_{fr} + i_{dr}) i_{qs} - L_m i_{qr} i_{ds} + (L_{ds} - L_{qs}) i_{ds} i_{qs}] \quad (9)$$

Because motor is use interior permanent magnet (IPM). So $L_{ds} \neq L_{qs}$, $i_{qr} = i_{dr} = 0$, $L_m i_{fr} = \lambda_f$. Therefore, according to (9) is expressed the follow equation [5].

$$T_e = \frac{3}{2}\frac{p}{2}[\lambda_f i_{qs} + (L_{ds} - L_{qs}) i_{ds} i_{qs}] \quad (10)$$

The mechanical torque equation is

$$T_e = J_m \frac{d\omega_r}{dt} + B_m \omega_r + T_L \quad (11)$$

where J_m is the moment of inertia of the motor, B_m is the viscous coefficient of the motor, T_L is the load torque, T_e is the motor torque, w_r is the mechanical rotor speed and equals to $w_e * \frac{2}{p}$, where P is the number of the poles.

3 Control methodology

This research presents the performance development of wide range high efficiency for electric propulsion system. The control block diagram of the proposed control strategy is depicted in Fig. 1.

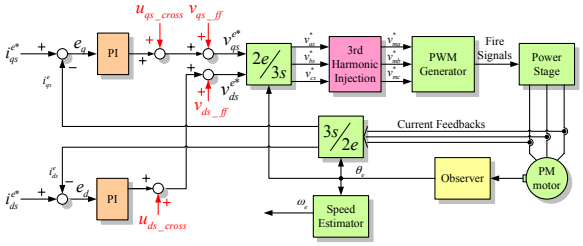

Figure 1: Control block diagram

3.1 Major Control Design

In this study, in order to achieve wide speed ranges high efficiency. First, there are two PI controllers which achieve current control of d-q axes. Secondly, feed-forward current control is introduced to compensate the performance of two PI current control outputs of d-q axes in overall operation range. Thirdly, the third harmonic injection is used to reduce computation complexity of a motor controller. Since simple computation of PWM signals, it can raise both rates of program execution and voltage utility. The detailed description of major control design is exhibited in the following subsections.

3.1.1 PI controllers

The two PI controllers have high steady-state precision; easy algorithm, good stability and high reliability. Define current error of d-q axes, $e_q = i_{qs}^{e^*} - i_{qs}^{e}$, and $e_d = i_{ds}^{e^*} - i_{ds}^{e}$. Therefore, two PI current control outputs of d-q axes can be written as

$$V_q = (K_p^p + \frac{K_I^p}{S}) e_q \quad (12)$$

$$V_d = (K_p^d + \frac{K_I^d}{S}) e_d \quad (13)$$

where K_p^p, K_p^d, K_I^p and K_I^d are control gains, S is Laplace operator.

3.1.2 Feed-forward current control

The feed-forward current control equations of d-q axes via feedback current, motor speed, stator inductance, stator resistance and flux linking can be written as

$$V_{qs\_ff} = r_s i_{qs}^{e^*} + \omega_e L_{ds} i_{ds}^{e^*} + \omega_e \lambda_f \quad (14)$$

$$V_{ds\_ff} = r_s i_{ds}^{e^*} - \omega_e L_{qs} i_{qs}^{e^*} \quad (15)$$

The cross couple control block diagram is depicted in Fig. 2. The cross couple control is introduced to compensate two PI current control error of d-q axes in overall operation range. It can be written as

$$U_{qs\_cross} = K_{cross}\omega_e (i_{ds}^{e^*} - i_{ds}^{e}) \quad (16)$$

$$U_{ds\_cross} = K_{cross}\omega_e (i_{qs}^{e^*} - i_{qs}^{e}) \quad (17)$$

where K_{cross} is cross couple gain.

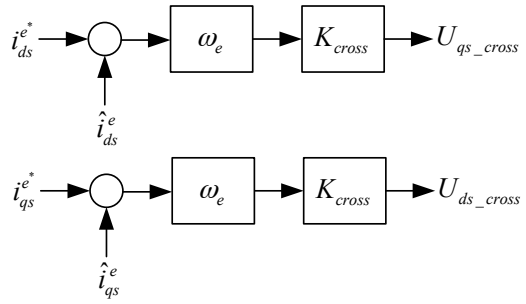

Figure 2: Cross couple control block diagram

3.1.3 Harmonic injection

In order to reduce computation complexity and raised voltage utility. Therefore, the third harmonic injection is used in the major control system. It is designed in Fig. 3, and can be written as

$$v_{harmonic} = -0.5(v_{max} + v_{min}) \quad (18)$$

$$v_{max} = \max\{v_{as}^*, v_{bs}^*, v_{cs}^*\} \quad (19)$$

$$v_{min} = \min\{v_{as}^*, v_{bs}^*, v_{cs}^*\} \quad (20)$$

$$\begin{aligned} v_{ma}^* &= v_{as}^* + v_{harmonic} \\ v_{mb}^* &= v_{bs}^* + v_{harmonic} \\ v_{mc}^* &= v_{cs}^* + v_{harmonic} \end{aligned} \quad (21)$$

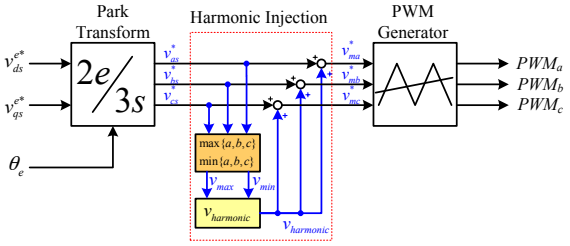

Figure 3: Harmonic injection control block diagram

4 Numerical simulation and experimental results

The detailed specifications of 50kW PMSM is shown in Table I.

Items	Specifications
Stator Outside Diameter	260 mm
Stator Inside Diameter	170 mm
Rotorr Inside Diameter	169 mm
Stack Length	90 mm
min. air gap length	1 mm
Tooth width	8 mm
Stator Yoke width	15.5 mm
Max. Power	50 kW
Max. Torque	210 Nm
Max. Speed	8000 rpm
Sensor Type	Resolver and Hall Sensor
Slot Number	42 slots
Pole Number	8 poles
Nominal DC bus voltage	300 V
Maximun DC bus voltage	336 V
Minimun DC bus voltage	192 V
Supply Peak AC Current	350 A

Table I: The detailed specifications of 50kW PMSM

4.1. Numerical simulation

In this paper all numerical simulations are carried out using Matlab/Simulink software. Figure 4 shows the simulated results of d-q axes current control for the PI control strategy. As can be seen from subfigures (a)-(b) of Figs. 4, favorable tracking responses can be obtained. But occurrence of the overshoot and transient response are serious.

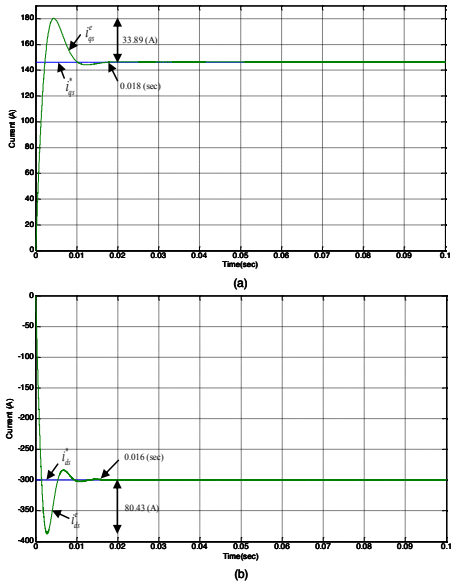

Figure 4: Control current of d-q axes for the PI control strategy

Figure 5 shows the simulated results of d-q axes current control for proposed control strategy. As can be seen from subfigures (a)-(b) of Figs. 5, favorable tracking responses can be obtained. From the simulated results in subfigures (a)–(b) of Figs. 5, the performance of the proposed control strategy can be achieved small occurrence of the overshoot and transient response. According to current of q axis in Fig. 4 (a) and Fig. 5 (a), the overshoot has 21 (A) improvements, and transient response has 0.006 (sce) improvements, in numerical simulations; than the PI control strategy. According to current of d axis in Fig. 4 (b) and Fig. 5 (b), the overshoot has 20 (A) improvements, and transient response has 0.006 (sce) improvements, in numerical simulations; than the PI control strategy. Consequently, the proposed control strategy is more suitable for electric propulsion system than the PI control strategy.

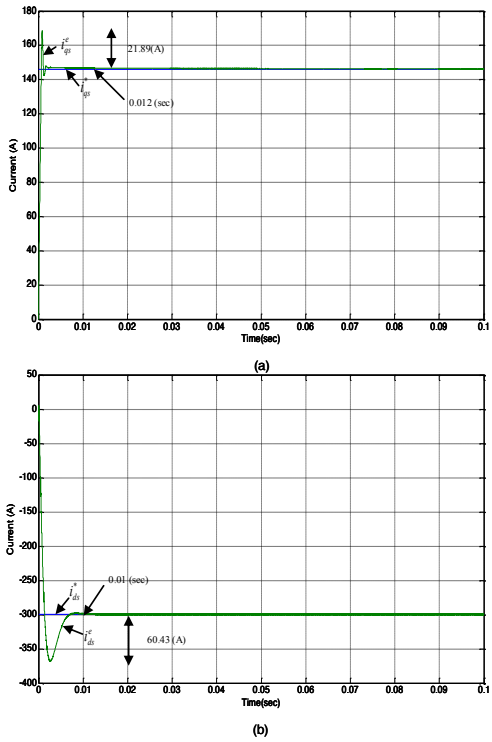

Figure 5: Control current of d-q axes for the proposed control strategy

4.2. Experimental results

In order to realize the value of the proposed control strategy in practical applications, a digital signal processor (DSP) F2808-based control platform is used for electric propulsion system. The electric propulsion system includes motor and controller. In the study, Fig. 6 shows the 50kW PMSM and Fig. 7 shows the motor controller. The picture of the experimental set-up for electric propulsion system is depicted in Fig. 8.

Figure 6: 50kW PMSM for this study

Figure 7: Motor controller for this study

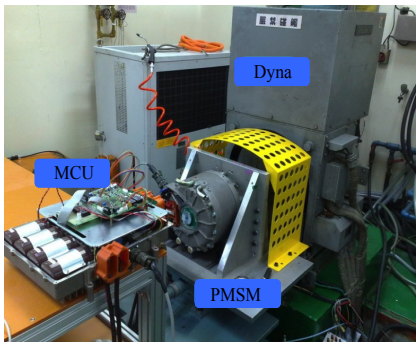

Figure 8: Picture of experimental set-up

This paper presents experimental results by a dynamometer. The experimental results include torque-speed curve as shown in Fig. 9, efficiency map as shown in Fig. 10, power and efficiency curves as shown in Fig. 11. Complete experiments guarantee the stability and the reliability of the electric propulsion system. From Fig. 9, the experimental result of torque-speed curve confirms that the maximum output torque of power module is 210 N.m. It is very obvious that good flux-weakening capability leads to wide speed range. We can got fine system performance in 3000~5000 rpm range as shown in Fig. 10.

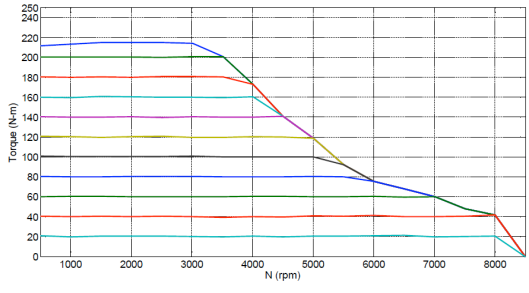

Figure 9: T-N curve

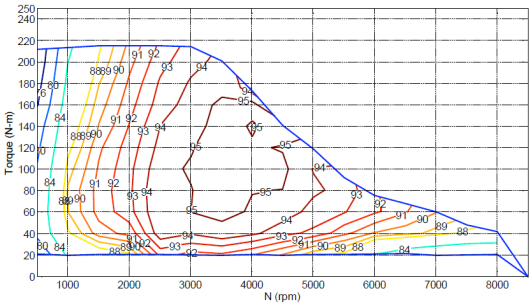

Figure 10: Efficiency map

In Fig. 11, the experimental results also verify that the wide range high efficiency of proposed control strategy is achieved for the electric propulsion system, and the system maximum efficiency is over 85% when normal rated power is 35kW. Power-efficiency curve also verify that the output power is about 44.8 kW in 2000~6000 rpm range; maximum output power is about 73.2kW at 3500 rpm. Efficiency is about 90.3% in 2000~6000 rpm range; maximum output efficiency is about 95.5% at 4500 rpm.

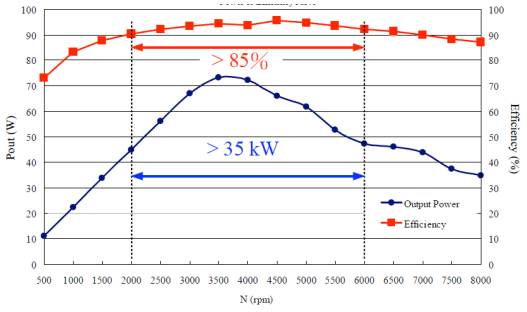

Figure 11: Power and efficiency curves

5 Conclusions

This paper successfully investigated feed-forward vector control strategy for 50kW PMSM. Through above-mentioned control strategy, the performance of PMSM can be enhanced for wide speed ranges high efficiency. The proposed control strategy resulted in the reducing of overshoot, transient response time and parameters tuning time; comparing with the PI current control strategy. Thus, the proposed control scheme is more suitable for electric propulsion system than the PI strategy. The major contributions of this study are summarized as follows. 1) The successful application of vector control mechanism and feed-forward current control strategy for the 50kW PMSM drive via a DSP considering the possible existence of uncertainties. 2) The idea of feed-forward current control strategy operation can be easily applied for other control systems.

Acknowledgments

The authors would like to acknowledge the financial support of Ministry of Economic Affairs (MOEA) of Taiwan, ROC, through grant number C353CC3100.

References

[1] W. H Li, et al., *Simulation research on optimization of permanent magnet synchronous motor sensorless vector control based on MRAS*, IEEE Press. 2012.

[2] B. K. Bose, *Power electronics and variable frequency drives-technology and application*, IEEE Press, 1997.

[3] R. J. Wai, et al, *Real-Time PID Control Strategy for Maglev Transportation System via Particle Swarm Optimization*, IEEE Trans. Vol. 58, no. 2, pp. 629-646, 2011.

[4] A. Mishra, et al, *Modeling and implementation of vector control for PM Synchronous motor Drive*, IEEE ICAESM, 2012.

[5] A. Mishra, et al, *Maximum Torque Control of IPMSM Drive with Multi-MFC*, IEEE International Conference on Control, Automation and Systems , 2010.

Authors

Kun-Lun Chuang was born in Hsinchu, Taiwan, R. O. C., in 1983. He received the B.S. degree in electrical engineering from Ming Hsin University of Science and Technology, Hsinchu, Taiwan, in 2006 and the M.S. degree in electrical engineering from Yuan Ze University, Taoyuan, Taiwan, in 2008. He is an engineer in Industrial Technology Research Institute, Hsinchu, Taiwan. His research interests include control theory applications and motor servo drives.

Dr. Yong-Kai Lin received the B.S., M.S., and Ph.D. degrees in electrical engineering from the National Taipei University of Technology, Taipei, Taiwan. He is currently an engineer in Mechanical and Systems Research Laboratories, Industrial Technology Research Institute, Hsinchu, Taiwan. His research interests include the field of fieldprogrammable gate array design and inverter control.

Dr. Shin-Hung Chang was born in Chung-Li, Taiwan, R. O. C., in 1979. He received the B. S. degree in electrical engineering from National Taiwan University of Science and Technology, Taipei, Taiwan, and the Ph. D. degree in electrical engineering from Yuan Ze University, Taoyuan, Taiwan, in 2002 and 2008, respectively. Since 2008, he has been a researcher and a project leader of EV key components in Industrial Technology Research Institute, Hsinchu, Taiwan. His research interests are intelligent, adaptive, and robust control theories and applications.

Mr. Bo-Tseng Sung was born in Taoyuan, Taiwan, R. O. C., in 1986. He received the B. S. degree in electronic engineering from Ta Hwa Institute of Technology, Hsinchu, Taiwan. He is an assistant engineer in Industrial Technology Research Institute, Hsinchu, Taiwan. His research interests are hardware design of motor controller, control and system integration.